Region Localization Using Recurrent Morphological Coding in Alzheimer MRI

Suresha H.S.[1], Dr. S.S. Parthasarathi[2]
[1]*Research Scholar, Don Bosco Institute of Technology, Department of ECE, Kumbalgodu, Mysore Road, Bangalore, India*
[2]*Professor, EEE Dept. PES Mandya*
(E-mail: srisuri75@gmail.com)

***Abstract*—**This paper presents an effective system for Alzheimer detection in Magnetic Resonance Imaging (MRI) scans using recurrent Gabor-morphological coding. While extracting the Alzheimer region in MRI scans, the problem of misclassification arises due to false detection of effective regions, which gives a semantic representation of Alzheimer region. The conventional approaches of Alzheimer detection based on morphological component analysis was used for its lower complexity and detection capabilities. However, the conventional approaches do not overcome the fundamental issues of scaling and orientation variations. To overcome this issue a recurrent model is suggested for Alzheimer detection. The experimental result illustrates the enhancements of the proposed approach over the conventional morphological component analysis

Keywords*—Alzheimer detection; Gabor-morphological component analysis; Magnetic resonance imaging; Recurrent modeling;*

I. INTRODUCTION

Automation in medical diagnosis has been in investigation for a long time. Researchers have focused on various aspects of medical data, such as automation of medical diagnosis, economical and accurate diagnosis. The primary objective of automated system is to overcome the dependency of sample analysis of the captured medical data and process in a supervised manner to extract and detect the effects observed in a given sample. Towards automation the various medical samples like MRI, Computed Tomography (CT), Electroencephalogram (EEG), mammogram, x-rays, Electrocardiography (ECG), etc. are analyzed in online or offline mode. To develop an automation approach for MRI analysis a similar objective of MRI diagnosis is also developed. In MRI detection, matched filtering is preliminary used for image pre-processing [1]. The matched filtering segments the Alzheimer regions in brain images that helps to define the different positions and orientation in MR images. However, the wrong choice of pre-processing approach leads to system complexity or overhead and loss of accuracy [2]. To address this issue, multi-threshold approaches are mostly preferred in Alzheimer detection. Generally, MRI used in two dimensional Gaussian filter blood pulse test for Alzheimer detection, which utilize neighborhood trigger neuron areas for simplifying and improving the segmentation process [3]. In a few researches, two dimensional Otsu thresholds are used for the detection of Alzheimer diseases. Here, Alzheimer final map was obtained through the analysis of regional connectivity. The wavelet transformation method is used for detecting abnormal MRI regions for obtaining good segmentation performance [4].

II. LITERATURE REVIEW

Several methodologies are developed by the researchers in Alzheimer detection. In this sub-section, a brief evaluation of a few essential contributions to the existing literature papers is presented.

In this paper, the data set has sensitivity of 0.7027 and 0.9717. Gabor wavelet and multilayered threshold based on a method is suggested. Gabor transformation wave boundary layer described are also described [5]. The suggested method and STARE and DRIVE data with an accuracy of 0.9 worked. Different width scale method for detecting Alzheimer's unit multi-scale approaches are outlined in this paper. A significant approach to detect Alzheimer line tracking multiple scales is suggested [6]. Method detection point process and standard brightness histogram and the test were invalid for the profiles of select seed has found. The purpose of the multi-scale approach to monitoring multiple scales, where the matrix of trust fine Alzheimer map was obtained through the use of derivative volume. In this paper, Average of 0.92-point accuracy, sensitivity of 0.74 and specificity of 0.95 are suggested and reached. Alzheimer's line of detection using a detection approach described in [7]. This method produces a line detector with different scales of infrastructure and that is developed based on the fact of varying lengths. Alzheimer's incredible final map was scaled by received integrating linear responses. The method was evaluated the DRIVE and STARE data sets and the average accuracy is 0.9407 and 0.9324 respectively. Pattern recognition methods are divided into two sub-sections. If the prior classification not occurred in Alzheimer monitoring methods, then the maps are used to generate some initial information. The feature vector consisting of image detail and description of the Gaussian filter combination is suggested. K-nearest neighbor method (KNN) was used to estimate the probability map [8]. Finally, the threshold probability map was created by Alzheimer's MRI [9]. The SVM method using radial projection was suggested for detection of Alzheimer's is based on self-training semi-supervised algorithm.

The method of detecting Alzheimer was suggested based on fuzzy. And it obtained average accuracy, sensitivity and specificity of 0.94, 0.74 and 0.97 in DRIVE data set, 0.94, 0.72 and 0.97 in STARE data set respectively [10]. In this method, in contrast to the first MR images using a matched filter, weighted fuzzy c-means clustering is a method used to identify structures with improved vascular tree. Pooling Gabor wavelet was used in 2-D and supervised classification to detect Alzheimer's MRI [11]. In [12] it outlined a method using an online operator and SVM classifier for categorizing pixels. Line operator, with the usual gray level was estimated permanent length of the lines of pixels in different directions. Estimation method is used for calculating the standard accuracy, which are 0.9563 and 0.9584 in DRIVE and STARE dataset respectively. Focus between two points using local details, Alzheimer fragmenting map tracking is used. Alzheimer's on the basis of the repeated fragmentation model is suggested [13]. Alzheimer method used to define the geometric properties of parametric model parameters. In Alzheimer's model-based approach, the MRI map was derived by applying a Twins ribbon model [14]. The method used the contours of the two pairs, while maintaining stability for the width of each side of the Alzheimer's capture [15]. The method was tested in the data set, and the obtained precision is, 0.9472 and 0.9567 in DRIVE and STARE respectively. In the blood of Alzheimer's in combination with topological properties was suggested based on the classical snake method for Alzheimer's detection [16]. For successful separation of the signal content analysis, enhancement and compression are required. They have outlined a series of expansion related to Alzheimer's [17-23]. A new method of morphological decomposition component analysis (MCA) is represented based on the signals are to have been outlined [24]. In MCA, it is assumed that each signal or morphological different layers of components, are distinguished by a linear combination of morphology. [25]. Morphological decomposition components (MCA) method is presented based on the signals it under-represented in a new analysis. It was assumed that each different signal layers in the MCA or morphological components are distinguished by a linear combination of morphology approach.

This paper proposed a new MRI blood Alzheimer's detection algorithm based on the recurrent morphological component analysis and Gabor transform. In this approach, Gabor filter gives all possible variations of the image in eight orientations. After obtaining all possible variations, the morphological operation is applied to separate the Alzheimer regions from the lesions. This paper is organized as follows: section II illustrates the details of the conventional approach, which applies the morphological operations directly on the MRI scans. Section III illustrates a brief review about the Gabor transform. Section IV gives the complete details about the proposed recurrent morphological model for Alzheimer detection. Experimental results are illustrated in section V and finally the conclusion is provided in section VI.

III. MRI ALZHEIMER DETECTION-MCA APPROACH

In MRI scan segmentation, the various approaches as outlined in the previous section in that the morphological approach has its own significance because of its lower computational complexity. A novel Alzheimer detection algorithm based on component separation is proposed [26]. The complete approach is carried out in three phases such as (1) preprocessing, (2) MR image cleaning and (3) Alzheimer segmentation.

A. Preprocessing

In the proposed approach, preprocessing selects the green channel MRI scans and better lighting, and also it eliminates the useless parts. Among the components of the color image, the green and red channel of the MRI scan is saturated with Alzheimer RGB background screens that represent the best contrast, and blue channel offers a poor dynamic range.

For this purpose, the green channel is selected by the MRI image. After getting the green channel of the MRI scan of interest, Otsu (ROI) algorithm is applied to the same area. MRIs are usually images, which is in the center surrounded by a black background it is called as a ROI. To detect Alzheimer's disease in processing steps, the ROI pixels should have accelerated after that, these useless parts are removed from the MRI. Morphological opening and closing are removed from the noisy areas. MRIs background changes due to non-uniform light intensity changes. This effect can degrade the performance of Alzheimer's segmentation algorithm.

B. MRI cleaning

MRI cleaning eliminates the noise and also detects the Alzheimer's erroneous. In addition, Alzheimer's can produce false positives in the final map. Then, apply MRI lesions Alzheimer's segmentation algorithm to remove the last of the Alzheimer's MRI to improve maps. In this approach, the MCA algorithm was applied to the lesions of separation. MCA candidate uses dictionaries algorithms to make it successful. Based on dictionaries, MCA algorithm separates Alzheimer's injuries. Dictionaries based on their structures are designed for both Alzheimer's.

In this paper, non-Sub sampled Contoured Transform (NSCT) conversion to Alzheimer's MRI images are used to represent different parts of the brain. Outline changes Sub samples (NSCT) help to choose the parts of lesion MRI images. In order to link the discontinuities of linear structures and directional filter banks to capture points the discontinuities uses Laplacian pyramid. Then, based on the Alzheimer algorithm different dictionaries MCA was applied to lesions. This is an iterative algorithm that setting a threshold for each dictionary Alzheimer fixing threshold and it also evaluates before fixing Alzheimer. In the first part of the algorithm, the fixed part of the lesion and Alzheimer's shared. The most important component of the lesion is removed and the residue is likely to include information and curved type structures which gives the representation for Alzheimer's. Then, a solution with the range and large selection coefficient can be achieved through hard thresholding limit coefficient. The initial price limit will automatically be adjusted to a sufficiently large value. In the next section, the similar steps are used for the components, i.e., the lesion part of a sub-dictionary, which hardly suits to select the specific structure representation.

C. Alzheimer Segmentation

After obtaining a clear MRI image, Alzheimer division tilt in all directions in response 0^0-180^0 is 20^0 selected with maximum modulus of the coefficients in a pitch angle is performed by applying wavelet Morlet changes. The Alzheimer's green channel inverted image is brighter than the background of the MRI scan before applying wavelet transform. However, the MR image is a one dimensional vector which is represented by wave decomposes Morlet. Then scale to improve the final image is calculated as the maximum modulus of the coefficients.

IV. GABOR TRANSFORMATION

Gabor filters have been featured in many works on image processing. However, analysis of these actions is related to the segmentation of assets. Directional multi-resolution decomposition was proposed linear images Gabor filters and tools used for the analysis. Directional multi-resolution images analysis Gabor filter, which is natural and desirable properties. Most of these properties described above are based on the study of biological vision. Multi-resolution analysis and image enhancement features such as partitioning and other techniques have been used successfully in the treatment of diseases. Exceeding a certain threshold value of the energy of a sub-image, the process of decomposition is applied, in decomposition steps. Many tree structures that rely heavily on the threshold value used. 2-D Gabor Gaussian function modulated by a complex sinusoid, which is mathematically denoted in the Eq. (1).

$$\psi(x,y)=\frac{1}{2\pi\sigma_x\sigma_y}\exp\left[-\frac{1}{2}\left(\frac{x^2}{\sigma_x^2}+\frac{y^2}{\sigma_y^2}\right)+2\pi jW_x\right] \quad (1)$$

Gabor wavelet zero bank balance reactions and generalized representation in DC is designed to reduce the redundancy of the filter which is shown in Eq. (1) and as a function of using dispersion and rotation $\psi(x,y)$ are obtained from parent represents,

$$\begin{aligned}&\psi_{m,n}(x,y)=a^{-m}\psi(x',y'),a>1,m,n=intege\\&x'=a^{-m}\left[(x-x_0)\cos\theta+(y-y_0)\sin\theta\right]\\&y'=a^{-m}\left[-(x-x_0)\sin\theta+(y-y_0)\cos\theta\right]\end{aligned} \quad (2)$$

Where (x_0,y_0) center of the filter in the spatial domain; $\theta=n\pi/K$ is denoted as the total number of orientations desired; and scale and orientation, respectively. The scale factor is meant to ensure that the energy is independent. Gabor wavelets in the frequency domain are defined in following Eq. (3).

$$\psi(u,v)=\frac{1}{2\pi\sigma_u\sigma_v}\exp\left\{-\frac{1}{2}\left[\frac{(u-W)^2}{\sigma_u^2}+\frac{v^2}{\sigma_v^2}\right]\right\} \quad (3)$$

The strategies used to filter project design, which ensures the average peak magnitude of reactions carried out in the area with architectural distortion field supports the filter in the frequency spectrum. Also, it ensures that the information capture filter with minimum redundancy. The obtained output for the gabor filter at different orientation reveals the orientation in one particular direction, an average gabor output is derived given by following Eq. (4).

$$K_{avg}=\left|\sum I(x,y)\right| \quad (4)$$

Where $I(x,y)$ is the Gabor output obtained at each orientation.

V. RECURRENT GABOR-MORPHOLOGICAL MODELING

In the selection of lesion regions from the obtained magnitude image the spectral variation in each orientation is observed. The spectral density varies at average density of 3-4 units in the Alzheimer region, whereas a spectral density variation with lesion region are observed to be at 1-2 variation. The extracted region is then further processed for lesion region extraction based on the directional filter-based approach. For the obtained spectral bands based on the Gabor output the orientation field, the details were derived and given by following Eq. (5),

$$\theta(x,y)=-\frac{\pi}{2}+K_{avg}\frac{\pi}{K} \quad (5)$$

The average estimated orientation field is then used for the designing of a directional filter for the estimation of the region, which is directionally different from the original region, as outlined in following section.

A. Directional Filtration Estimation

Directional filter estimation (DFE) for image processing directional flow is expected. The main asset of a directional filter information directional 2D image that shows the orientation of the image content and image analysis and other applications have the ability to extract important. This is a classification of such institutions, removing images, better recognition and fingerprint images, as has been used in various imaging applications. The applications such as, feature classification, image denoising, fingerprint image enhancement and recognition, etc. The directional filter is characterized by maximally decimated and perfect reconstruction property without losing the image generality. It is implemented by a tree structure consisting of three levels of two-band systems. Each level stage polyphase filter is removable, which makes it extremely computationally efficient structure can be implemented. For the extracted average Gabor output the directional filter is applied to extract the 2D- directional variations on which the region of interest is extracted. The filtered input image usually has smooth regions with feature regions variation at distorted and non-distorted region. Directional shift, a filter bank of eight channels, with a tree structure, consisting of three phases is proposed to achieve. At

each stage, the image filter and a filter bank are decimated by two channels. The tree structure used in the matrices Q1 down-sampling, D0 and D1 are. Step 3. Finally, a number eight sub-band (almost) equal samples are obtained by decomposition. To obtain a set of filter output, S = {1, 2, 3, 4, 5, 6, 7, 8}, the index modulation defines the directional sub-band, M = 8 Directional number of bands, indicates problem designed with an objective function can be formulated as an optimization problem, which is given by following Eq. (6).

$$\phi = \sum_{j=0}^{M-1} \left(\sum_n f_j(-n) h_j(n) - 1 \right)^2 \quad (6)$$

The cost function is optimized for the selected filter based on the defined pass band support. The filter structure for the directional filter is expressed by Eq. (7).

$$h(k)_i = \frac{1}{2}\left(h_0\left(\theta/2\right) + h_0\left((\theta - 2\pi/2)\right)\right) \quad (7)$$

Where k is represented as the iteration for filtration and θ is the obtained orientation field for a given sample. The generic 8 orientations are obtained for the selected directional filter for tracing, which is graphically denoted in the Fig. 1.

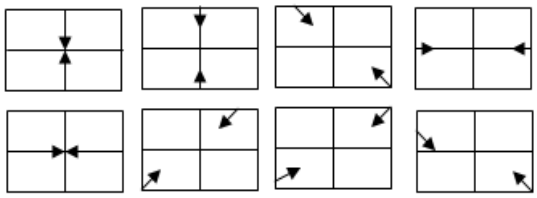

Figure 1. 8 Directional filter orientations for the estimation.

The overall implementation for the suggested approach is summarized as,

Algorithm:

1) Read the input sample.
2) Apply Gabor filtration with 180 orientations at uniform step. Eq. (3)
3) Compute the average Gabor output. Eq. (4)
4) Compute the orientation field θ. Eq. (5)
5) Define a directional filter $h(k)_j$ for the obtained θ. Eq.(7)
6) Apply the directional filter on the extracted spectral map output.
7) Compute the cost function of the developed filter output. Eq. (6)
8) repeat the iteration to converge the cost function.
9) obtained direction map at the lowest cost function is one direction region extracted

Alzheimer received eight areas and is a logical shift operation, as illustrated by using the global threshold logic for each orientation is organizing a two-level figure. Range is a simple technique for image segmentation. Objects or areas of the image as the background are different. Areas and regions showed that the areas of Alzheimer's, are formed by resolution detail each component is also true that the intensity of the non-Alzheimer's Alzheimer areas prestigious areas. Therefore, an early non-Alzheimer's resolution to remove components sectors the sub-bands can select an appropriate category. On the border with neighboring pixels, each pixel value T target range value as a dynamic range value is calculated from an equation is obtained. Each pixel mask equation is used to calculate the threshold value for the two operators in order to receive offers. In fact, for different purposes, different dynamic range of the threshold value method receives resolution images. Each component is not to resolve a binary image resolution. The range is determined by T, which is given in Eq. (8).

$$T = \frac{\sum\left(e_s(i,j) X_s(i,j)\right)}{\sum s(i,j)} \quad (8)$$

Where,

$$S(i,j) = \max\left(\left|g_1 ** e_s(i,j)\right| \left|g_2 ** e_s(i,j)\right|\right) \quad (9)$$

and,

$$g_1 = [-101], g_2 = [-101]^t \quad (10)$$

In Eq. (9), "* *" denoted as two-dimensional linear convolution.

Fig. 2 shows an example of a determination factor $5\times5(es)$. The matrix in the form of Equation -9 and the 69masking matrix elements (P 8) is calculated by,

$$\begin{pmatrix} p_1 & p_2 & p_3 & p_4 & p_5 \\ p_6 & p_7 & p_8 & p_9 & p_{10} \\ p_{11} & p_{12} & p_{13} & p_{14} & p_{15} \\ p_{16} & p_{17} & p_{18} & p_{19} & p_{20} \\ p_{21} & p_{22} & p_{23} & p_{24} & p_{25} \end{pmatrix}$$

Figure 2. 5×5 resolution component sub-band *(es)*

$$s(p_g) = \max\left(|p_9 - p_7|, |p_{13} - p_3|\right) \quad (11)$$

Each pixel implementing similar operations, elements $S(i,j)$ for each component sub-band solution. Equation 8,

limit the T , and binary (e) Using the image edge can be calculated and it is represented in the following Eq. (12).

$$e(i,j)=\begin{cases}255, & if\ e_s(i,j)>T\\ 0 & otherwise\\ & 1\end{cases} \quad (12)$$

Orientation to eliminate the influence of noise between a set of proposals for an error correlation is assumed. Consider a set of $K(OK)$ given a set of image data to a set of $i=1$ to M shown in Eq. (13).

$$O_i(k)=\left[O_i(kN),(kN-1).....O_i(kN-M+1)\right] \quad (13)$$

Where O_i , resolution of a particular orientation, N is the number of orientations and M samples of the data set. The defined orientation fault is calculated to assess the effect of noise, which is shown in Eq. (14).

$$e_{i,o}(k)=O_{i,t}(k)-O_{i,t+1}(k) \quad (14)$$

This error component orientation and orientation to minimize errors in the difference of two values $\left(e_{i,o}(k)\right)$ is regarded as an element of the unit defines minimum. But when observed over a period of observation, orientation and noise impact of this error is a result of straying can be effective. Therefore, the orientation will be concentric with the intersection coding noise parameter. To eliminate this problem, and to improve the selection of the right pixels, morphological spectrum turns to calculate a series of orientation is calculated a selection. The suggested approach, but all the histogram information from a single orientation, is a selection of bars to resolution. Select the resolution to get the solution was initially a random factor using the weight normalized interval, which is given by following Eq. (15).

$$O_i(k)=O_i(k)w(k) \quad (15)$$

Where, $w(k)=\left[w_0(k),w_1(k),.....w_{M-1}(k)\right]^T$ are the allocated weight factor for each frame. The estimated error is then defined by the following Eq. (16).

$$e_{i,o}(k)=O_{i,t}(k)-O_i(k)w(k) \quad (16)$$

The error is recursively been computed over the total orientations $(i=1....N)$, and the initial error is recorded as $e_{i,o,\text{init}}$. A weight factor is then updated by using the following Eq. (17),

$$w(k+1)=w(k)+\mu\sum_{i=0}^{N-1}\frac{o_i^T(k)}{\left\|o_i(k)\right\|^2}e_{i,o,init}(k) \quad (17)$$

Where, μ is an updation factor error is updated with a step size. The purpose of this calculation condition min $\left(e_{i,o,}(k)\right)$ the meeting of the selection of the bins. Recursive to optimize overhead, a weight defined by the adjacent joint is calculated using the Eq. (18).

$$W(k)=w^o-w(k) \quad (18)$$

Where W_o initial weight continues. Weight update again that is defined in the Eq. (19).

$$W(k+1)=W(k)-\mu\sum_{i=0}^{N-1}\frac{O_i^T}{\left\|uO_i(k)\right\|^2}e_{i,o}(k) \quad (19)$$

B. Logical AND Operation

Alzheimer's enhanced image data and logic operations to isolate three types of morphological operations (vertical, horizontal and diagonal) are available. Logical AND operator element for element operation performed three images and get the final image (ANDED). The operations of morphology resulting in the removal of graph area used when the graphic area ANDED greater uniformity than in Alzheimer's.

VI. EXPERIMENTAL RESULTS & DISCUSSION

For experimental simulation, MATLAB (version 2013) was employed on PC with 3.2 GHz with i5 processor. The proposed Alzheimer algorithm was applied to the dataset. Preprocessing phase worthless pieces of MRIs were eliminated. The green channel MRI showed the resized image 512 x 512 pixels and uneven light output through the image preprocessing filter obtained in Step 30 is shown in Fig. 2.

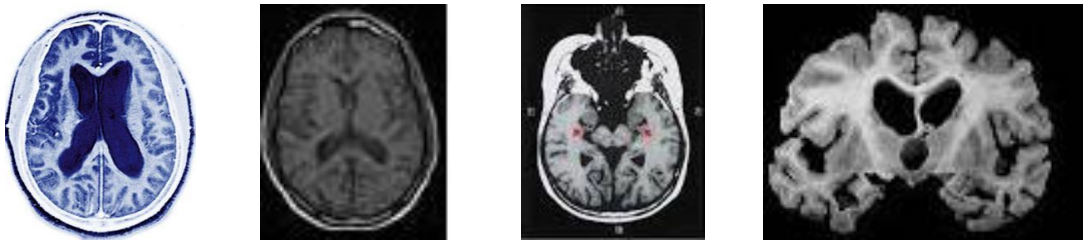

(a) (b) (c) (d)

Figure.2. (a) Original image, (b) Green plane extracted image, (c) Cropped region and (d) Illumination enhanced image

In the next phase, the proposed approach through enhanced image Gabor transform to distinguish Alzheimer's lesions was applied.

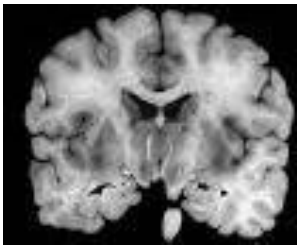

Figure.3. Gabor orientation resolution components

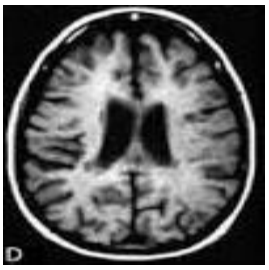

Figure.4. Selected top four morphalized image for Gabor resolution

Figure.5. Extracted Alzheimer regions on performing logical AND

The approach developed the following parameters are used to evaluate performance, which is shown following Eq. (20).

$$Accuracy = \frac{TP + TN}{TP + TV + FP + FN} \tag{20}$$

Where,

$TP = True\ positive\left(Correctly\ identified\right)$

$FP = False\ positive\left(Incorrectly\ identified\right)$

$TN = True\ negative\left(\ false, Correctly\ identified\right)$

$FN = False\ negative\left(\ false, incorrectly\ identified\right)$

Compared to previous approaches, the proposed approach shows more sensitivity and specificity, which were evaluated using the following mathematical expression. Sensitivity positive that are correctly identified as such in the ratio is measured in Eq. (21).

$$Sensitivity = \frac{TP}{TP + FN} \tag{21}$$

Specification negatives are correctly identified as such in the ratio is measured in the equation (22).

$$Specificity = \frac{TN}{TN + FP} \tag{22}$$

MR images of the proposed approach and precision, sensitivity and specificity of the proposals was tested on ten samples which are shown in the following table 1. A comparative analysis of the proposed GMCA former MCA is represented in the following table 1. The proposed method is shown at DRIVE minimum and maximum data values are highlighted in bold set the performance measurement images. The proposed method is compared with existing methods in terms of accuracy, sensitivity and specificity and which is shown in Fig. 7, 8 and 9.

TABLE I. PERFORMANCE METRICS OVER TEN SAMPLES

Sample	Accuracy		Sensitivity		specificity	
	MCA[26]	GMCA	MCA[26]	GMCA	MCA[26]	GMCA
S1	0.9541	0.9727	0.7558	0.7685	0.9775	0.9733
S2	0.9542	0.9645	0.7061	0.7241	0.9871	0.9875

S3	0.9492	0.9874	0.7228	0.7342	0.9808	0.9856
S4	0.9553	0.9745	0.7550	0.7684	0.9828	0.9842
S5	0.9513	0.9558	0.7140	0.7198	0.9756	0.9867
S6	0.9474	0.9586	0.7058	0.7256	0.9770	0.9854
S7	0.9483	0.9491	0.7815	0.7985	0.9600	0.9701
S8	0.9424	0.9542	0.7861	0.7952	0.9644	0.9725
S9	0.9474	0.9678	0.7632	0.7752	0.9728	0.9756
S10	0.9524	0.9632	0.7150	0.7412	0.9769	0.9798

In addition, the proposed method performance characteristic curve for receptor (ROC) behavior is measured. An ROC curve the True Positive (TP), False Positives (FP) versus fraction represents. TP, whereas Alzheimer FP, not misidentified as part of pixels correctly identified as part of Alzheimer's disease. The Area under Curve (AUC) is used to characterize the optimal behavior of the system, which is equal to 1. Fig. 6 shows that the proposed approach is optimal because the proposed approach is fast, when compared with the previous MCA.

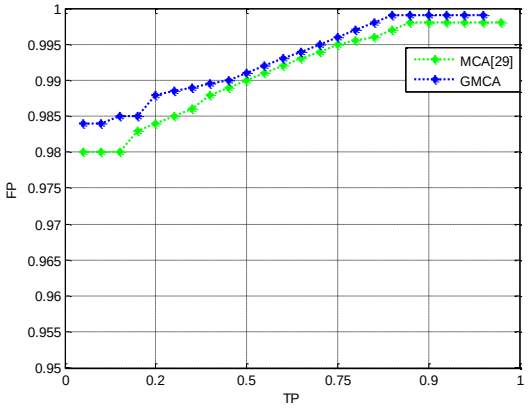

Figure.6. ROC plot

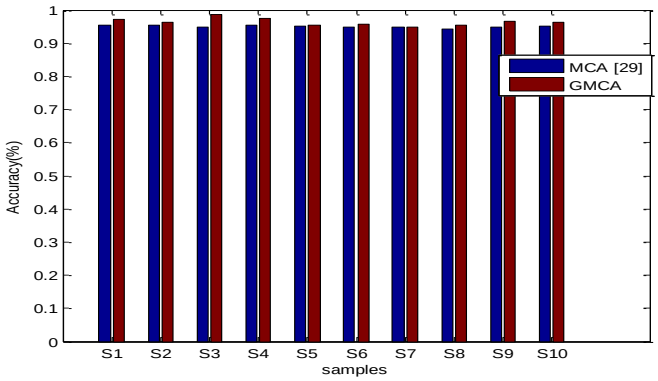

Figure.7. Accuracy of different samples for MCA and GMCA

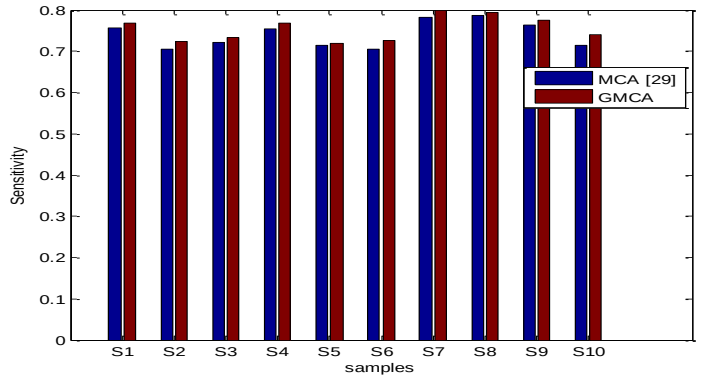

Figure.8. Sensitivity of different samples for MCA and GMCA

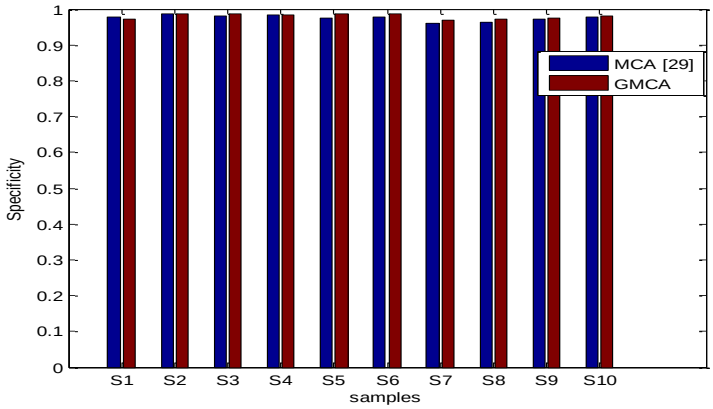

Figure.9. Specificity of different samples for MCA and GMCA

Fig. 7 illustrates the accuracy resolutions of the proposed work. The accuracy of proposed method is high compared to earlier approaches since the proposed GMCA finds out all the possible variations in the Alzheimer detection such that the proposed approach effectively segments the all Alzheimer's from the MRI images.

Sensitivity reflects the ability of an approach to find out the correct values. In this approach, the sensitivity can be defined as the ability of approach to segment the Alzheimer's correctly. The sensitivity plot for the proposed GMCA and the earlier MCA algorithms is shown in fig. 8. Likewise, from the Fig. 9, the specificity of the proposed approach is observed to be high compared to MCA, thus the GMCA can efficiently detect the blood Alzheimer's form MRI images.

VII. CONCLUSION

In this paper, Gabor transformation algorithm and morphological components are presented for Alzheimer's detection. These components analysis the unusual symptoms of Alzheimer's that gives greater ability for removing lesions from the MRI scans. Therefore, pre-processed images for the detection of Alzheimer's the MRI maps were drawn. So, MRI improves the Alzheimer's map by the result of the eliminating affected divisions. Alzheimer's blood with signs of diabetic retinopathy has the ability to find the blocks in the blood vessels.

REFERENCES

[1] B. Sangmesh, and A. S. Jadhav, "A Survey on Blood Alzheimer Segmentation and Optic Disc Segmentation of MRI Images," InternationalJournal of Advanced Research in Computer and Communication Engineering, vol. 4, 2015.

[2] B. Nishu, "MRI Alzheimers Detection Algorithm for Biomedical Symptoms Diagnosis," International Journal of Computer Applications, 2013.

[3] S. H. Wang, Y. Zhang, Y. J. Li, W. J. Jia, F. Y. Liu, M. M. Yang, and Y. D. Zhang, "Single slice based detection for Alzheimer's disease via wavelet entropy and multilayer perceptron trained by biogeography-based optimization," Multimedia Tools and Applications, pp.1-25, 2018.

[4] Y. Zhang, S. Wang, Y. Sui, M. Yang, B. Liu, H. Cheng, J. Sun, W. Jia, P. Phillips, and J. M. Gorriz, "Multivariate approach for Alzheimer's disease detection using stationary wavelet entropy and predator-prey particle swarm optimization," Journal of Alzheimer's Disease, vol.65, pp. 855-869, 2018.

[5] J. Siva Kumar, K. Chitra, "Segmentation of Blood Alzheimers Using Improved Line Detection And Entropy Based Thresholding," Journal of Theoretical and Applied Information Technology, vol. 63, 2014.

[6] V. Marios, and E. Dermatas, "Multi-scale MRI Alzheimer segmentation using line tracking," computerized medical imaging and graphics, vol. 34, 2010.

[7] H. Yanli, "Automatic Segmentation of MRI Blood Alzheimers Based onImproved Multiscale Line Detection," Journal of Computing Science and Engineering, vol. 8, 2014.

[8] M. Deepa, "Comparative analysis on supervised classification techniques for segmentation and detecting abnormal blood Alzheimers in MRI images," International Conference on Emerging Trends in Science, Engineering and Technology (INCOSET), 2012.

[9] P. C. Siddalingaswamy, and K. Gopalakrishna Prabhu, "Automatic Segmentation of Blood Alzheimers in Colour MRI Images using Spatial Gabor Filter and Multiscale Analysis," ICBME, springer 2008.

[10] M. E. Jayasingh, and S. Allwin, "Supervised Algorithm based Blood Alzheimer Segmentation in MRI Images," International Journal of Digital Content Technology and its Applications (JDCTA), vol. 9, 2015.

[11] A. K. Razieh "A Novel MRI Blood Alzheimer Segmentation Algorithm using Fuzzy segmentation," International Journal of Electrical and Computer Engineering (IJECE) vol. 4, 2014.

[12] R. Ghaderi, "MRI Alzheimer segmentation using the 2-D Morlet wavelet and neural network," International Conference on Intelligent and Advanced Systems, ICIAS, 2007.

[13] R. Jegatha, "MRI Blood Alzheimer Segmentation using Gray-Level and Moment Invariants-Based Features," Journal of Computer Applications ISSN: 0974 – 1925, vol. 5, 2012.

[14] D. Selvathi, and L. Vaishnavi, "MRI Blood Alzheimer Segmentation Using Gabor Wavelet and Support Vector Machine," International Journal of Neural Networks and Applications, vol. 4, 2011.

[15] A. B. Xiaohong Gao, A Method of Alzheimer Tracking for Alzheimer Diameter Measurement on MRI Images," IEEE 2001.

[16] Z. Yitian, L. Rada, K. Chen, S. P. Harding, and Y. Zheng, "Automated Alzheimer Segmentation Using Infinite Perimeter Active Contour Model with Hybrid Region Information with Application to MRI Images", IEEE Transactions On Medical Imaging, Vol. 34, No. 9, September 2015.

[17] D.SivaSundhara Raja, "Performance Analysis of MRI Image Blood Alzheimer Segmentation", Advanced Computing: An International Journal (ACIJ), Vol.5, No.2/3, May 2014.

[18] L. Espona, M.J. Carreira, M. Ortega, M.G. Penedo, "A snake forMRI Alzheimer segmentation," in: Pattern Recognition andimage Analysis, Springer, Berlin Heidelberg, 2007.

[19] Kamala Devi.K, Agnes Anto, K.John Peter, "Curvelet Transform and Multi Structure Elements Morphology by Reconstruction based MRI Image Analysis," International Journal of Soft Computing and Engineering (IJSCE) ISSN: 2231-2307, volume-2, 2012.

[20] H. Gehad, "MRI blood Alzheimer segmentation approach based on mathematical morphology," International Conference on Communication, Management and Information Technology (ICCMIT), 2015.

[21] M. Schweda, A. Kögel, C. Bartels, J. Wiltfang, A. Schneider, and S. Schicktanz, "Prediction and Early Detection of Alzheimer's Dementia: Professional Disclosure Practices and Ethical Attitudes," Journal of Alzheimer's Disease, vol. 62, pp. 145-155, 2018.

[22] E. Chaitanya, "Sparse Decomposition Of Transformation-Invariant SignalsWith Continuous Basis Pursuit," Proc Int'l Conf Acoustics Speech Signal Processing (ICASSP), Prague, Czech Republic, 2011.

[23] P. M. Rodrigues, D. R. Freitas, J. P. Teixeira, D. Alves, and C. Garrett, "Electroencephalogram Signal Analysis in Alzheimer's Disease Early Detection," International Journal of Reliable and Quality E-Healthcare (IJRQEH), 7(1), pp.40-59, 2018.

[24] F. G. Meyer, A. Z. Averbuch, R. R. Coifman, "Multilayered imagerepresentation: application to image compression," IEEETrans. Image Process, vol. 11, 2002.

[25] Y. Meyer, "Oscillating patterns in image processing andnonlinear evolution equations, in: The fifteenth deanjacqueline," B. Lewis memorial lectures, vol. 22, amsbookstore, 2001.

[26] I. Elaheh, "Improvement of MRI blood Alzheimer detection using morphological component analysis," ELSEVIER, Computer methods and programs in bio-medicine, 2015.